Nuclear magnetic resonance studies of motion and structure of cubic liquid crystalline phases

ARTICLE *in* THE JOURNAL OF PHYSICAL CHEMISTRY · FEBRUARY 1982

Impact Factor: 2.78 · DOI: 10.1021/j100392a021

3 AUTHORS:

Per-Olof Eriksson
AstraZeneca
27 PUBLICATIONS **649** CITATIONS
SEE PROFILE

Ali Akhtar Khan
21 PUBLICATIONS **840** CITATIONS
SEE PROFILE

Göran Lindblom
Umeå University
232 PUBLICATIONS **7,769** CITATIONS
SEE PROFILE

Nuclear Magnetic Resonance Studies of Molecular Motion and Structure of Cubic Liquid Crystalline Phases

Per-Olof Eriksson,† Ali Khan,‡ and Göran Lindblom*

Division of Physical Chemistry, University of Umeå, S-901 87 Umeå, Sweden, and Division of Physical Chemistry 2, Chemical Centre, University of Lund, S-220 07 Lund, Sweden *(Received: June 2, 1981; In Final Form: October 2, 1981)*

The ^{14}N spin–lattice (T_1) and spin–spin (T_2) relaxation times in the cubic phases of the dodecyltrimethylammonium chloride ($C_{12}TAC$)–water and hexadecyltrimethylammonium fluoride ($C_{16}TAF$)–water systems, the ^{14}N quadrupole splittings in the hexagonal phases, and the amphiphile diffusion coefficient in the cubic phases were measured as functions of temperature. Diffusion measurements show that the cubic phase at 84% $C_{12}TAC$ and the cubic phase of the $C_{16}TAF$ system consist of aggregates which are continuous over macroscopic dimensions whereas the cubic phase at 50% $C_{12}TAC$ consists of globular amphiphile aggregates. The NMR results can be explained with a model where the molecular motion is divided into a fast, locally anisotropic mode of motion and a slow, isotropic mode of motion. The correlation time of the slow motion, τ_c^s, is interpreted in terms of the lateral diffusion coefficient. From τ_c^s and the measured diffusion coefficient of the cubic phase, an estimate of the dimension of the cubic unit cell is obtained. The structural parameter so determined is in good agreement with X-ray data.

Introduction

Lyotropic liquid crystalline phases generally form at high amphiphile concentrations.[1] The structure of the lamellar and hexagonal phases are well established while the structures of the various cubic phases[2-4] are still under study. In recent years much attention has been paid to these isotropic phases, due to their importance in particular biology, since they have been observed in bile systems,[5] in so-called prolamellar bodies in chloroplasts,[6] in membranes,[7] and in mixtures of membrane lipids from *Acholeplasma laidlawii*.[8]

The structures of the cubic phases have been investigated mainly by X-ray and NMR. In the pioneering X-ray work of Luzzati and co-workers,[9-11] several different structures were proposed and determined (cf. Figure 1). The remarkable structure consisting of rod-shaped aggregates connected three by three building up a three-dimensional network was later supported by NMR diffusion studies of Charvolin and Rigny.[12] These authors found that the amphiphile molecules were able to diffuse over macroscopic distances, and therefore a structure composed of close-packed spherical micelles could be ruled out.

NMR diffusion coefficients[13] of dodecyltrimethylammonium chloride ($C_{12}TAC$) in the micellar solution and in two different cubic phases of the $C_{12}TAC$–water system (cf. Figure 2) indicated that one of these cubic phases consisted of close-packed spheres while the other one contained continuous hydrocarbon regions. Later it was shown by one of us[14-16] and co-workers that NMR diffusion methods are very powerful and quantitative information about aggregate structure of cubic phases may be obtained. The geometry of the aggregates building up the cubic phases can be determined from a quantitative comparison between the translational diffusion coefficients of the cubic phases and the lamellar phase in the same system. This is possible since the diffusion coefficient in the lamellar phase can be *directly* measured[14,17] by NMR, i.e., without using probe molecules, or by measurements of parameters that are only *related* to the diffusional motion. Recently it was suggested[18] that also very sensitive polarized fluorescence methods could be used for the investigation of the aggregate structure of cubic phases.

In this work we have studied cubic liquid crystalline phases in the binary systems $C_{12}TAC$–water and hexadecyltrimethylammonium fluoride ($C_{16}TAF$)–water (for phase diagram see preceeding article) using several different NMR techniques. A thorough analysis of the ^{14}N relaxation times in terms of slow and fast motions in the amphiphile aggregates is performed. It is shown that, from measurements of relaxation times, amphiphile diffusion coefficients and quadrupole splittings for appropriate phases of the systems, information about aggregate structure, and an estimation of the dimension of the unit cell can be extracted for the cubic phases.

Materials

Hexadecyltrimethylammonium fluoride was prepared

† Division of Physical Chemistry, University of Umeå.

‡ Division of Physical Chemistry 2, Chemical Center, University of Lund.

* Address correspondence to this author at the following address: Division of Physical Chemistry, University of Umeå, S-901 87 Umeå, Sweden.

(1) P. E. Ekwall, "Advances in Liquid Crystals", Vol. 1, G. H. Brown, Ed., Academic Press, New York, 1975, p 1.
(2) V. Luzzati and A. Tardieu, *Annu. Rev. Phys. Chem.*, **25**, 79 (1974).
(3) K. Fontell, *Prog. Chem. Fats Other Lipids*, **16**, 145 (1978).
(4) G. J. T. Tiddy, *Phys. Rep.*, **57**, 1 (1980).
(5) J. S. Patton and M. C. Cary, *Science*, **204**, 145 (1979).
(6) B. E. S. Gunning, *Protoplasma*, **60**, 111 (1965).
(7) A. Stier, S. A. Finch, and B. Bösterling, *FEBS Lett.*, **91**, 109 (1978).
(8) Å. Wieslander, L. Rilfors, L. B.-Å. Johansson, and G. Lindblom, *Biochemistry*, **20**, 730 (1981).
(9) V. Luzzati and P. A. Spegt, *Nature (London)*, **215**, 701 (1967).
(10) V. Luzzati, A. Tardieu, Y. Gulik-Krzywicki, E. Rivas, and F. Reis-Husson, *Nature (London)* **220**, 485 (1968).
(11) A. Tardieu and V. Luzzati, *Biochim. Biophys. Acta*, **219**, 11 (1970).
(12) J. Charvolin and P. Rigny, *J. Magn. Reson.*, **4**, 40 (1971).
(13) T. Bull and B. Lindman, *Mol. Cryst. Liq. Cryst.*, **82**, 155 (1974).
(14) G. Lindblom and H. Wennerström, *Biophys. Chem.*, **6**, 167 (1977).
(15) G. Lindblom, K. Larsson, L. B.-Å. Johansson, K. Fontell, and S. Forsén, *J. Am. Chem. Soc.*, **101**, 5465 (1979).
(16) G. Lindblom, *Acta Chem. Scand., Ser. B*, **35**, 61 (1981).
(17) G. Lindblom, L. B.-Å. Johansson, and G. Arvidson, *Biochemistry*, **20**, 2204 (1981).
(18) L. B.-Å. Johansson and G. Lindblom, *Q. Rev. Biophys.*, **13**, 63 (1980); *J. Chem. Phys.*, in press.
(19) K. Fontell, *J. Colloid Interface Sci.*, **43**, 156 (1973).
(20) L. E. Scriven, *Nature (London)*, **263**, 123 (1976).
(21) R. R. Balmbra, J. S. Clunie, and J. F. Goodman, *Nature (London)*, **222**, 1159 (1969).

0022-3654/82/2086-0387$01.25/0

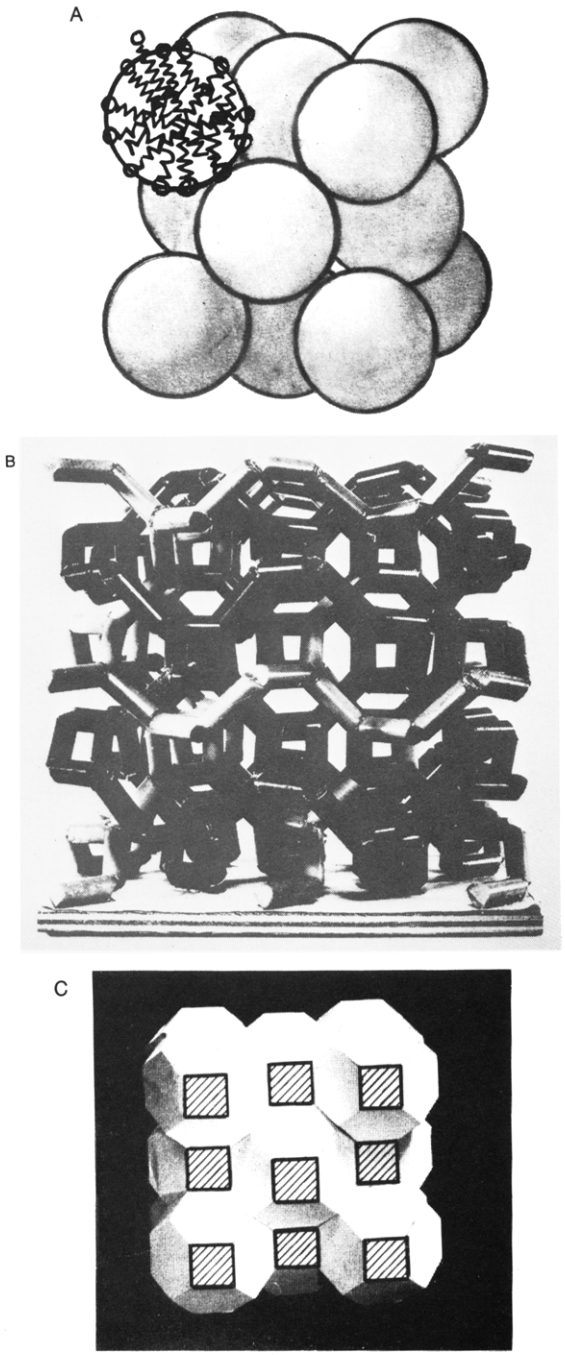

Figure 1. Some proposed structure models for cubic liquid crystalline phases of amphiphile and water. (A) A cubic phase structure consisting of close-packed micellar aggregates surrounded by water. The amphiphile molecules are restricted to move within the aggregates. (B) A cubic phase structure consisting of two interwoven but otherwise independent networks of rodlike amphiphile aggregates surrounded by water. The phase structure is "bicontinuous"; i.e., both the amphiphile and the water molecules are free to move over macroscopic distances. Note that the rods in the picture represent only the axes of the aggregates; the length and the diameter of the aggregates are almost the same.[19] (C) A "bicontinuous" cubic phase structure composed of open tetrakaidecahedra. The hexagon-shaped surfaces represent the lipid bilayer units, and the shaded surfaces represent the water channels.[15]

as described elsewhere.[22] Dodecyltrimethylammonium chloride was purchased from Eastman Kodak Co. and was used without further purification. Heavy water (99.7 at. % ^2H) was purchased from Ciba-Geigy, Switzerland.

(22) A. Khan, K. Fontell, and G. Lindblom, *J. Phys. Chem.*, preceeding paper in this issue.

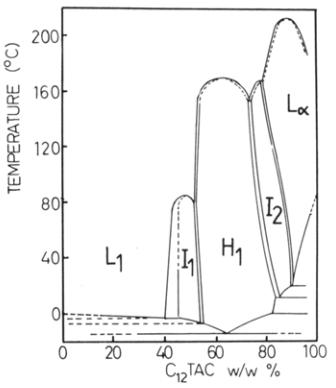

Figure 2. Phase diagram of the dodecyltrimethylammonium chloride (C_{12}TAC)–water system: (L_1) isotropic solution, (H_1) normal hexagonal liquid crystal, (L_α) lamellar liquid crystal, (I_1 and I_2) cubic liquid crystalline phases (from ref 21).

The samples were prepared by weighing appropriate amounts of amphiphile and water into glass tubes which were sealed off. Mixing was accomplished by repeated heating and centrifuging for 2–3 days. The samples were kept standing for at least 1 week before any measurements were made. Unless otherwise stated, heavy water was used. The ^2H NMR spectrum of the samples consisted of a single isotropic line (cubic phases) or of a single splitting with no isotropic signal (hexagonal phases), which affirmed the homogeneity of the samples. Before measurements were performed on cubic samples, the optical isotropy was confirmed by observation of the sample through crossed polarizing glasses.

Methods

Diffusion Measurements. The diffusion coefficient of the amphiphile in the cubic phases of the C_{16}TAF and C_{12}TAC systems was determined with the pulsed magnetic field gradient technique developed by Stejskal and Tanner.[23] A Bruker 322s pulsed NMR spectrometer equipped with a home-built digitalized pulsed magnetic field gradient unit was used. The 60-MHz proton spin echo was monitored at time 2τ after a 90°–τ–180° rf pulse sequence. When pulsed field gradients are applied at each side of the 180° rf pulse, molecular diffusion will attenuate the spin echo at 2τ according to

$$\ln E/E_0 = -(\gamma g \delta)^2(\Delta - \delta/3)D \qquad (1)$$

where E/E_0 is the echo attenuation, γ is the magnetogyric ratio, and D is the molecular diffusion coefficient.

The magnitude of the gradient pulses, g, and the time spacing, Δ, between them were kept constant while the duration, δ, of the gradient pulses was varied. Typical settings were ~1.0–2.0 T m^{-1} for g, 20 or 30 ms for τ, and 26 or 39 ms for Δ. δ was varied between 0 and 8 ms, and the echo amplitude was measured several times on an oscilloscope. The diffusion coefficient, D, was calculated from the slope of a plot of $\ln E/E_0$ against $\delta^2(\Delta - \delta/3)$. The magnetic field gradients were calibrated by measurements on glycerol.[24] The diffusion coefficient of heavy water in the cubic samples was determined from the ^2H spin echo attenuation, pure heavy water being used for calibration.[25] The probe temperature was controlled by a heated airflow around the sample tube and measured by using a copper/constantan thermocouple placed in a tube of the same type as the sample tubes. The samples were thermally

(23) E. O. Stejskal and J. E. Tanner, *J. Chem. Phys.*, **49**, 288 (1965).
(24) D. J. Tomlinson, *Mol. Phys.*, **25**, 735 (1973).
(25) R. Mills, *J. Phys. Chem.*, **77**, 685 (1973).

TABLE I: Measured Amphiphile Diffusion Coefficients (D) for Cubic Phases in the $C_{16}TAF$ and $C_{12}TAC$ Systems and Lateral Diffusion Coefficients of the Amphiphile in Some Lamellar Liquid Crystalline Phases

sample	compn, wt %	phase	temp, °C	$10^{11}D$, $m^2\ s^{-1}$
$C_{16}TAF$[a]	75.0	cubic	59	2.5
^2H_2O	25.0		65	3.2
			71	4.3
			75	4.8
$C_{12}TAC$[b]	84.0	cubic	26	0.76
^2H_2O	16.0		36	1.2
			47	2.0
			57	2.6
			67	3.6
			78	5.0
			87	6.7
$C_{12}TAC$	50.1	cubic	47	<0.2
^2H_2O	49.9			
C_8SO_4Na[c]	30.9	lamellar	24	3.5[e]
$C_{10}OD$	35.8			
^2H_2O	33.3			
C_7COONa	22.0	lamellar	24	21[e]
$C_{10}OD$	40.0			
^2H_2O	38.0			
C_8NH_3Cl	72.0	lamellar	24	33[e]
^2H_2O	28.0			
NaAOT[d]	60.0	lamellar	24	2.7[e]
^2H_2O	40.0			

[a] $C_{16}TAF$ = hexadecyltrimethylammonium fluoride. [b] $C_{12}TAC$ = dodecyltrimethylammonium chloride. [c] Alkyl chains are written as C_x where x denotes the number of carbon atoms in the chain. [d] NaAOT = sodium diethylhexyl sulfosuccinate (sodium salt of Aerosol OT). [e] The lateral diffusion coefficient, D_L (from ref 14).

equilibrated for at least 1 h before measurements were performed.

Relaxation Time Measurements. ^{14}N spin relaxation times in the cubic phases of the $C_{12}TAC$ system were measured at a resonance frequency of 18.418 MHz by using a home-built pulsed Fourier transform spectrometer equipped with an Oxford Instruments 6 T wide bore magnet. For the cubic phase of the $C_{16}TAF$ system, ^{14}N measurements were made on a modified Varian XL-100-15 pulsed Fourier transform spectrometer at 7.229 MHz. The longitudinal relaxation time, T_1, was measured by the inversion recovery technique and was calculated by a three-parameter least-squares fit of the equation $M_z(\tau) = M_0[1 - k\ \exp(-\tau/T_1)]$ to the data. $M_z(\tau)$ is the signal amplitude at a delay time of τ between pulses, M_0 is the equilibrium magnetization, and k is equal to 2 for a perfect 180° rf pulse. The transverse relaxation time, T_2, was obtained from the line width at half-height, $\Delta\nu_{1/2}$, of the resonance signal. The measured line width, $\Delta\nu_{1/2}$, was corrected for the contribution from the magnetic field inhomogeneity, $\Delta\nu_{1/2}$(inhom), by the relation $(\pi T_2)^{-1} = \Delta\nu_{1/2} - \Delta\nu_{1/2}$(inhom). $\Delta\nu_{1/2}$(inhom) was taken as the line width at half-height of the ^{14}N NMR signal from a concentrated aqueous solution of $N(CH_3)_4Cl$, having a negligible natural line width.

Typical settings for the experimental parameters were as follows: number of transients, 5000 (for line width measurements) and 1000 (for T_1 measurements); signal length, 20 ms; and spectrum width, 10 kHz. The waiting time between pulse sequencies in the T_1 measurements was at least $5T_1$.

Measurements of ^{14}N Quadrupolar Splitting. The ^{14}N splittings in the hexagonal phase of the $C_{16}TAF$ and $C_{12}TAC$ systems were measured at a resonance frequency of 18.418 MHz. Typical settings were as follows: number of transients, 30 000; spectrum width, 30 kHz; pulse duration, 30 μs; signal length, 20 ms; and total waiting time between pulses, 50 ms.

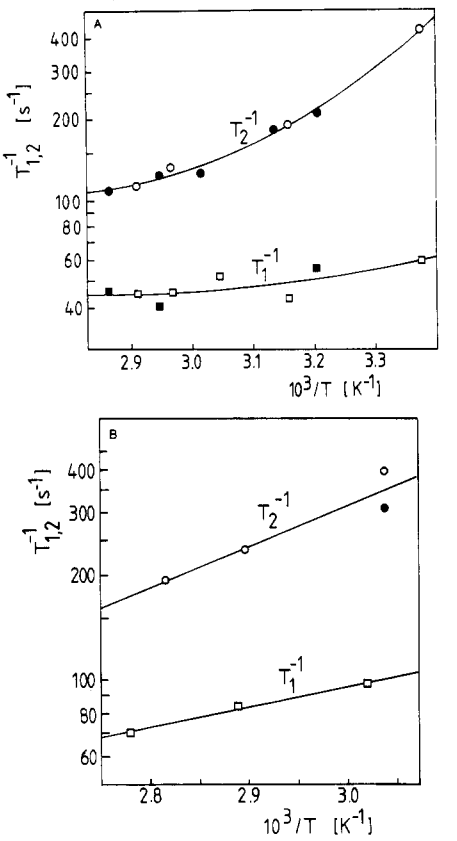

Figure 3. (A) The ^{14}N spin–spin (T_2^{-1}) (O, ●) and the spin–lattice (T_1^{-1}) (□, ■) relaxation rates plotted against the inverse of the absolute temperature in the cubic phase at low water content in the $C_{12}TAC$ system. Sample composition: (O, □) 84.0 wt % $C_{12}TAC$, 16.0 wt % ^2H_2O; (●, ■) 84.4 wt % $C_{12}TAC$, 15.6 wt % ^1H_2O. (B) The ^{14}N spin–spin (T_2^{-1}) (O, ●) and the spin–lattice (T_1^{-1}) (□) relaxation rates plotted against the inverse of the absolute temperature in the cubic phase of the $C_{16}TAF$ system. Sample composition: (O, □) 80.8 wt % $C_{16}TAF$, 19.2 wt % ^2H_2O; (●) 75.0 wt % $C_{16}TAF$, 25 wt % ^2H_2O.

TABLE II: ^{14}N Spin-Lattice (T_1^{-1}) and Spin-Spin (T_2^{-1}) Relaxation Rates for a Cubic Liquid Crystalline Sample Containing 49.3 wt % $C_{12}TAC$ and 50.7 wt % ^2H_2O at 18.418 MHz

temp, °C	T_1^{-1}, s^{-1}	T_2^{-1}, s^{-1}
23	42	273
43	32	107

Results

The amphiphile diffusion coefficient was measured at various temperatures for the cubic phases (cf. Figure 2 and ref 22) of the $C_{12}TAC$ and $C_{16}TAF$ systems. The results are given in Table I together with some previously published amphiphile diffusion coefficients in lamellar phases. The amphiphile diffusion coefficient in the cubic phase of the $C_{16}TAF$ system and in the cubic phase at 84% $C_{12}TAC$ gave linear Arrhenius plots with activation energies of 38.6 and 31.2 kJ mol^{-1}, respectively. The water (^2H_2O) diffusion coefficient of the cubic samples was at least 1 order of magnitude greater than the amphiphile diffusion coefficient. This clearly shows that the contribution from free ^1H_2O to the ^1H amphiphile spin echo is negligible. T_1 and T_2 of ^{14}N for the cubic phases determined as functions of temperature are given in Figure 3, A and B, and in Table II. The ^{14}N quadrupole splitting as a function of temperature for the hexagonal phases is given in Figure 4.

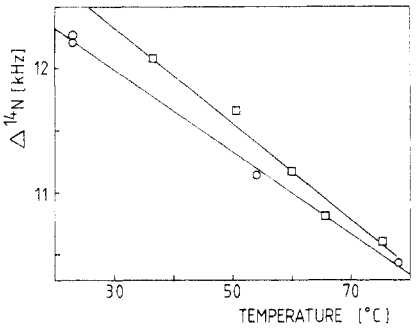

Figure 4. ^{14}N quadrupole splitting as a function of temperature in the hexagonal phase of the $C_{12}TAC$ system and of the $C_{16}TAF$ system. Sample composition: (□) 45.2 wt % $C_{16}TAF$, 54.8 wt % ^2H_2O; (○) 63.3 wt % $C_{12}TAC$, 36.7 wt % ^2H_2O.

Discussion

Diffusion Measurements. The NMR method with pulsed magnetic field gradients constitutes a direct way of measuring the diffusion coefficient in lipid systems.[14,23,26] As the experimental diffusion time corresponds to displacements over colloidal dimensions, the NMR diffusion method gives indications of any restriction for translational motion in the system. For example, a diffusion time of 50 ms and a diffusion coefficient of 10^{-11} m^2 s^{-1} corresponds to a root mean square displacement of 1700 nm, which is well above the dimension of a micelle. This makes the NMR diffusion method useful for structural investigations of cubic liquid crystalline phases.

We have previously shown that amphiphile diffusion coefficients can give information about the aggregate structure of cubic phases.[14-16] This information is extracted from a comparison between the coefficients determined for the lamellar and cubic phases. For the cubic phase the diffusion measurements are made straightforwardly, while for lamellar phases the samples have to be macroscopically aligned and oriented at the so-called magic angle relative to the magnetic field.[27]

It is well established[13,14,28] that there exist two fundamentally different types of cubic mesophases (cf. Figure 1), those having discrete hydrocarbon regions, like close-packed globular micelles, and those having a continuous hydrocarbon region extending over macroscopic distances in three dimensions. The amphiphile molecule is free to move within the aggregates, but it is highly unlikely[14] that it will pass over an aqueous region into an adjacent aggregate. Therefore, although the local molecular diffusion probably is the same, a cubic phase with discontinuous hydrocarbon regions will have a measured diffusion coefficient well below that of a lamellar sample.[14-16] On the other hand, in a cubic structure consisting of continuous hydrocarbon regions, the amphiphile molecule can move over macroscopic distances without passing through an aqueous region. The macroscopic diffusion coefficient will then be of the same order as that of oriented lamellar samples.

As seen from Table I, the measured lipid diffusion coefficient of the cubic phase of the $C_{16}TAF$ system[22] and of the cubic phase at 80% $C_{12}TAC$ (cf. Figure 2) are of the same order of magnitude as those found in lamellar phases of other systems. Therefore, these cubic phases most probably consist of aggregates which are continuous over macroscopic distances. However, the cubic phase at 50% $C_{12}TAC$ has an amphiphile diffusion coefficient considerably smaller than those found in the other two cubic phases or in lamellar phases. We therefore conclude that this phase consists of noncontinuous aggregates, probably globular aggregates. Similar results have also been published previously.[13]

Relaxation Time Measurements. For a nucleus with spin greater than one-half, the NMR spectrum is dominated by the interaction between the nuclear quadrupole moment and the electric field gradient at the nucleus.[29] This interaction depends upon the relative orientation of the principal axis systems of the nuclear quadrupole and the field gradient tensors. The field gradient tensor is fixed in the molecule. The quadrupole moment tensor, on the other hand, is fixed relative to the external magnetic field. Molecular reorientation will therefore modulate the interaction, and the NMR spectrum is determined by the strength of the interaction and by the time scale at which it is modulated. If, within a time which is short compared to the inverse of the static interaction, the distribution of molecular orientations is isotropic, the static quadrupole interaction is averaged out and a single line appears in the spectrum.

Usually the quadrupole interaction provides the dominant mechanism of spin relaxation. If the group containing the observed nucleus has at least a threefold symmetry axis, as the group $CH_2N^+-(CH_3)_3$, the asymmetry parameter of the electric field gradient tensor, $\eta = (V_{xx} - V_{yy})/V_{zz}$, is zero. V_{xx}, V_{yy}, and V_{zz} are the components of the electric field gradient tensor in its principal axis system. Then for a spin one nucleus, as ^{14}N, the longitudinal (T_1) and transverse (T_2) spin relaxation times can be written[29]

$$\frac{1}{T_1} = \frac{3\pi^2}{40}\chi^2\{2\tilde{J}(\omega_0) + 8\tilde{J}(2\omega_0)\} \quad (2a)$$

$$\frac{1}{T_2} = \frac{3\pi^2}{40}\chi^2\{3\tilde{J}(0) + 5\tilde{J}(\omega_0) + 2\tilde{J}(2\omega_0)\} \quad (2b)$$

Here ω_0 is the Larmor frequency, χ is the quadrupolar coupling constant defined as eQV_{zz}/h where eQ is the nuclear quadrupole moment, V_{zz} is the largest component of the electric field gradient tensor expressed in its principal axis system, and h is Planck's constant. $\tilde{J}(\omega)$ is a reduced spectral density function.[29]

If the molecular motion can be described by a single correlation time, τ_c

$$\tilde{J}(\omega) = 2\tau_c/[1 + (\omega\tau_c)^2] \quad (3)$$

Equations 2 and 3 predict that, as the correlation time decreases with increasing temperature, either $T_1 = T_2$ and both T_1 and T_2 increase (extreme narrowing $\omega_0\tau_c \ll 1$) *or* $T_1 \neq T_2$, T_2 increases, and T_1 decreases ($\omega_0\tau_c \gg 1$). Our data on T_1 and T_2 given as a function of temperature do not fit into that pattern (cf. Figure 3 and Table II). As the temperature is increased, both T_1 and T_2 *increase* while at the same time $T_1 \neq T_2$. This discrepancy can, however, be explained by a simple model as follows.

The cubic phases investigated here show no quadrupolar splittings and are thus characterized by overall isotropy on the NMR time scale. It is clear, however, that the reorientation of the amphiphile head groups must be *locally* anisotropic. To account for the effect of this local anisotropy on the spin relaxation, we will adopt a simple and physically reasonable model[28,30,31] comprising two

(26) E. O. Stejskal, *Adv. Mol. Relaxation Processes*, 27, 3 (1972).
(27) G. Lindblom, *Acta Chem. Scand.*, 261, 1745 (1972).
(28) J. Charvolin and P. Rigny, *J. Chem. Phys.*, 58, 3999 (1973).
(29) A. Abragam, "The Principles of Nuclear Magnetism", Oxford University Press, London, 1961.
(30) H. Wennerström, G. Lindblom, and B. Lindman, *Chem. Scr.*, 6, 97 (1974).
(31) B. Halle and H. Wennerström, *J. Chem. Phys.*, 75, 1928 (1981).

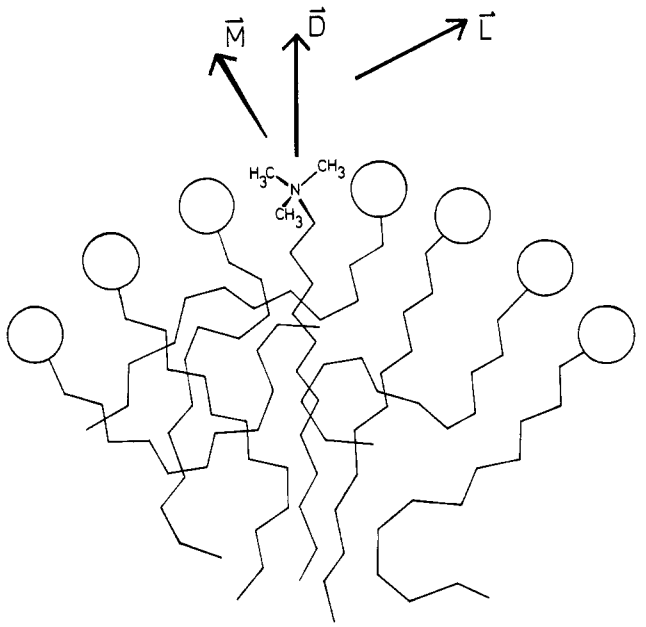

Figure 5. Schematic drawing of the aggregate surface of a lyotropic liquid crystalline phase. L denotes a laboratory-fixed axis, D is the normal to the aggregate surface, and M is the threefold symmetry axis through the nitrogen nucleus in the amphiphile molecule.

modes of motions, namely, a fast one and a slow one.

Denote (cf. Figure 5) the normal to the surface of the aggregate by D, the molecular symmetry axis through the nitrogen nucleus by M, and a laboratory-fixed axis by L. The fast mode consists of a rapid anisotropic reorientation of M relative to D. The slow motion is determined by the translational diffusion along the surface of the aggregate, thereby reorienting D relative to L.

The time scales of the fast and slow motions have to be sufficiently different so that the angle between D and L remains essentially constant when the angle between M and D is statistically averaged (i.e., the molecules go through all orientations of the local orientational distribution). The quadrupolar interaction is partially averaged out by the fast motion, which gives rise to a residual anisotropy. This is characterized by a local order parameter, S, defined as the ensemble average of $^1/_2(3\cos^2\beta - 1)$ where β is the time-dependent angle between M and D. It is assumed that the orientational distribution of M around D has at least a threefold symmetry. In the cubic phase the residual interaction, χS, is then completely averaged out by the diffusional motion along the aggregates. Then, it can be shown[30,31] that

$$\tilde{J}(\omega) = (1 - S^2)\tilde{J}_f(\omega) + S^2\tilde{J}_s(\omega) \quad (4)$$

where $\tilde{J}_f(\omega)$ and $\tilde{J}_s(\omega)$ are the reduced spectral densities characterizing the fast motion and the slow motion, respectively.

From T_2 and T_1 (cf. eq 2), information about the slow motion can be extracted. Assuming extreme narrowing conditions for the fast mode, ($\tilde{J}_f(0) = \tilde{J}_f(\omega_0) = \tilde{J}_f(2\omega_0)$), we find from eq 2 and 4

$$\frac{1}{T_2} - \frac{1}{T_1} = \frac{9\pi^2}{40}\chi^2S^2[\tilde{J}_s(0) + \tilde{J}_s(\omega_0) - 2\tilde{J}_s(2\omega_0)] \quad (5)$$

If the slow motion can be described by a single correlation time, τ_c^s, eq 5 becomes

$$\frac{1}{T_2} - \frac{1}{T_1} = \frac{9\pi^2}{20}\chi^2S^2\left\{\tau_c^s + \frac{\tau_c^s}{1 + (\omega_0\tau_c^s)^2} - \frac{2\tau_c^s}{1 + 4(\omega_0\tau_c^s)^2}\right\} \quad (6)$$

TABLE III: Correlation Times for the Fast (τ_c^f) and Slow (τ_c^s) Motions of the Head Group of the Amphiphile in the Cubic Phase Containing 49.3 wt % C_{12}TAC and 50.7 wt % ^2H_2O, Calculated According to Eq 9 and 10, and the Radius, R, of the Globular Aggregates Calculated According to Eq 11[a]

temp, °C	$10^{10}\tau_c^f$, s	$10^8\tau_c^s$, s	R, nm
23	3.7	4.8	2.5
43	1.1	1.6	2.1

[a] T_1^{-1} and T_2^{-1} of ^{14}N are taken from Table II, and interpolated values of the ^{14}N quadrupolar splitting in the hexagonal phase of C_{12}TAC and water, $\Delta_{hexagonal}$, are taken from the line drawn in Figure 4. The lateral diffusion coefficient of the amphiphile, D_L, is taken as $3D_{measured}$ from the cubic phase of 84 wt % C_{12}TAC and 16 wt % $2H_2O$.

Thus, knowing χS, one can calculate τ_c^s from T_1 and T_2.

In anisotropic systems, like hexagonal or lamellar phases, the molecular motion will not average the quadrupolar interaction[30,31] to zero. As for isotropic systems, the fast local motion leads to a partial averaging of the interaction from χ to χS. The residual interaction then gives rise to a quadrupolar splitting in the NMR spectrum. For a powder sample, where all microcrystallite orientations are represented, the quadrupole splitting for the spin one nucleus case is[30]

$$\Delta = {}^3/_4|\chi S| \quad (7)$$

In a hexagonal phase the molecules diffuse rapidly around the cylindrical aggregates. If the local environment of the molecule is independent of aggregate shape, it can be shown[28,30] from symmetry arguments that the motion around the aggregates brings about a halving of the quadrupole interaction. This has also been confirmed experimentally by a number of workers.[28,32-35] It is therefore reasonable to assume that the local environment of a molecule in the aggregates of a cubic phase is the same as in a lamellar or hexagonal aggregate of the same system. The residual quadrupole interaction, χS, is then

$$|\chi S| = {}^4/_3\Delta_{lamellar} = {}^8/_3\Delta_{hexagonal} \quad (8)$$

From T_1 and T_2 of ^{14}N in the cubic phases in the C_{16}TAF and C_{12}TAC systems and from ^{14}N quadrupolar splittings of the hexagonal phases, the correlation time, τ_c^s, for the *slow motion* is calculated from

$$\tau_c^s\left\{1 + \frac{1}{1 + (\omega_0\tau_c^s)^2} - \frac{2}{1 + 4(\omega_0\tau_c^s)^2}\right\} = \frac{5}{16\pi^2}\left(\frac{1}{T_2} - \frac{1}{T_1}\right)\frac{1}{\Delta_{hexagonal}^2} \quad (9)$$

Interpolated values of the measured parameters are used in order to refer to the same temperature. In Tables III and IV calculated values of τ_c^s are given at different temperatures.

(32) U. Henriksson, L. Ödberg, and J. C. Eriksson, *Mol. Cryst. Liq. Cryst.*, **30**, 73 (1975).
(33) Å. Wieslander, J. Ulmius, G. Lindblom, and K. Fontell, *Biochim. Biophys. Acta*, **512**, 241 (1978).
(34) G. W. Stockton, C. F. Polnaszek, A. P. Tulloch, F. Hasan, and I. C. P. Smith, *Biochemistry*, **15**, 954 (1976).
(35) H. Wennerström and J. Ulmius, *J. Magn. Reson.*, **23**, 431 (1976).
(36) U. Henriksson, L. Ödberg, J. C. Eriksson, and L. Westman, *J. Phys. Chem.*, **81**, 76 (1977).

TABLE IV: Correlation Times for the Fast (τ_c^f) and Slow (τ_c^s) Motions of the Head Group of the Amphiphile in the Cubic Phase at 84% C_{12}TAC and in the Cubic Phase in the C_{16}TAF System, Calculated from Eq 9 and 10[a]

compn (wt %)	temp, °C	$10^{10}\tau_c^f$, s	$10^8\tau_c^s$, s	R_{rod}, nm	$R_{lamellar}$, nm	$d/2$, nm
C_{12}TAC (84%)-water (16%)	22					3.95[b]
	23	6.0	7.6	3.1	2.2	
	40	4.3	3.6	3.0	2.1	
	50	3.6	2.6	3.1	2.2	
	60	3.2	2.1	3.3	2.3	
	68	3.0	1.9	3.6	2.5	
	76	3.0	1.8	3.9	2.8	
C_{16}TAF (81%)-water (19%)	55	6.8	6.0	4.8	3.4	
	65	4.8	4.7	5.3	3.7	
	70					4.93[c]
	75	3.2	3.7	5.7	4.0	

[a] $R_{rod/lamellar}$ of a sphere inscribed in the cubic unit cell was calculated from eq 11. T_1^{-1} and T_2^{-1} of ^{14}N are taken from the lines drawn in Figure 3. The ^{14}N quadrupole splitting in the hexagonal phase, $\Delta_{hexagonal}$, is taken from the lines drawn in Figure 4. For comparison, X-ray data on the parameter d of the cubic unit cell is given. In the assumed model for the molecular motion $d/2$ should be equal to R. [b] From ref 3 and 21. [c] $d/2$ for C_{16}TAB from ref 10.

Likewise, if the fast motion can be described by a single correlation time, τ_c^f, eq 2a, 3, and 4 give

$$\frac{1}{T_1} = \frac{3\pi^2}{10}\chi^2\left\{5(1 - S^2)\tau_c^f + S^2\left(\frac{\tau_c^s}{1 + (\tau_c^s\omega_0)^2} + \frac{4\tau_c^s}{1 + 4(\tau_c^s\omega_0)^2}\right)\right\} \quad (10)$$

where we have assumed extreme narrowing conditions for the fast motion ($(\tau_c^f\omega_0)^2 \ll 1$). The quadrupole coupling constant has been estimated[36] to be χ = 83.5 kHz. $|S|$ can then be calculated from eq 8, and the correlation time for the fast motion is obtained from eq 10. Tables III and IV give τ_c^f at different temperatures. It is found that the fast motion obeys extreme narrowing conditions ($\omega_0\tau_c^f$ is less than 0.1), a prerequisite for eq 5 and 10. Furthermore, τ_c^s is about 100 times greater than τ_c^f, which gives further support for the model used. Hence, the spin–lattice relaxation time is mainly determined by the fast motion while the spin–spin relaxation is dominated by the slow motion.

Interpretation of τ_c^s and Cubic Phase Structure. The correlation time for the slow motion, τ_c^s, can be interpreted in terms of the diffusional motion along the aggregate surface and/or the rotational motion of the whole aggregates. Consequently, the structure of the cubic phase must have a great influence on the value of τ_c^s. Simple relations between correlation time, diffusion coefficient, and the geometry of the aggregate have been derived, and the correlation time for diffusion on a *spherical surface* is given by[29]

$$\tau_c^d = R^2/(6D_L) \quad (11)$$

where R is the radius of the sphere and D_L is the lateral diffusion coefficient on the surface. Thus, for a cubic phase consisting of close-packed spheres (Figure 1) which do not rotate, an estimate of R can be obtained from measurements of τ_c^s and D_L. Previously, we have shown[14-16] that D_L can be measured with the pulsed magnetic field gradient methods in lamellar samples. Assuming that the translational diffusion within the aggregates does not depend on the aggregate shape,[14-16] D_L in eq 11 can be taken from such measurements. Unfortunately, however, there is no lamellar phase in the C_{16}TAF system,[22] and, since the lamellar phase region is very narrow at low temperatures in the C_{12}TAC system (cf. Figure 2), it is difficult to macroscopically align a lamellar sample for this system. However, the translational diffusion coefficient can be conveniently measured for a cubic phase[13-15] consisting of continuous amphiphile aggregates. Furthermore, a lateral diffusion coefficient can also be estimated for an assumed geometry of the aggregates (lamellar or rod) building up the cubic phase. For a detailed description of this, see ref 14 and 15. Here we only quote the results; namely, for a cubic phase with rodlike aggregates the *measured* diffusion coefficient $D = {}^1/_3D_L$ and for a cubic phase with lamellar units $D = {}^2/_3D_L$.

Since there is restricted diffusion in the cubic phase at 50% C_{12}TAC, it can be expected to consist of globular aggregates. The lateral diffusion coefficient can, on the other hand, be obtained from the cubic phase at 84% C_{12}TAC for which a rodlike aggregate structure has been assumed. In Table III calculated values of R on this basis for the cubic phase at 50% C_{12}TAC are given at two temperatures. Due to uncertainties in the measured quantities, the error in the R values is estimated to be about 15%. The radius of a globular aggregate should not be longer than the full all-trans length of the amphiphile molecule i.e., about 1.8–1.9 nm. Since chloride counterions and some water molecules probably diffuse together with the amphiphiles, the R values obtained are in excellent agreement with globular aggregates. From X-ray investigations the radius of the cylindrical aggregates of the hexagonal phase is 1.8 nm,[22] which also is compatible with the R values for the cubic phase. If, on the other hand, lamellar units are assumed for the cubic phase at 84% C_{12}TAC, the R values in Table III will be smaller by a factor of $\sqrt{2}$, leading to unrealistically small aggregates. Thus, the following conclusions can now be drawn. The slow correlation time, τ_c^s, is determined by the diffusional motion, and the cubic phase at 50% C_{12}TAC consists of globular aggregates with a radius of about the full length of the amphiphile. Moreover, the NMR data indicate that the cubic phase with 84% C_{12}TAC contains rodlike aggregates (cf. also below).

Bicontinuous Cubic Phase Structures. For a cubic phase consisting of globular aggregates, the interpretation of τ_c^s is straightforward, while for the amphiphile-continuous cubic phases it is more difficult. In the latter case the molecular motion takes place on a complicated, three-dimensionally folded surface, which extends over macroscopic dimensions. For the residual quadrupolar interaction to be averaged out completely, the amphiphile molecules have to take on all possible orientations in the cubic unit cell in a time which is short compared with the inverse of the residual interaction. Assuming that the diffusional motion can be described by a single correlation time, this would depend on the lateral diffusion coefficient in a similar manner as in eq 11. The denominator comes from the fact that the interaction is described by a second

rank tensor[29] and would therefore be the same. The numerator depends upon the structure and dimension of the aggregates and would be proportional to the square of the dimension of the cubic unit cell.

A useful *model*, for which simplicity is the chief justification, for the translational motion in these isotropic liquid crystalline phases is that it occurs on a sphere inscribed in the cubic unit cell. In this model $2R$, as given by eq 11, determines the dimension of the cubic unit cell. As described above, for a cubic phase consisting of rodlike aggregates, $D_L = 3D_{measured}$, and, for lamellar aggregates, $D_L = {}^3/_2 D_{measured}$. Thus, the method gives different values of R depending on the structural model. Through a comparison with X-ray diffraction data on the dimension of the cubic unit cell, it is possible to discriminate between the two models.

In Table IV calculated values of R are given for the cubic phase at 84% C_{12}TAC and the cubic phase in the C_{16}TAF system assuming rod- or lamellar-shaped aggregates. As can be seen from Table IV, calculated values of R are in better agreement with X-ray investigations assuming a rodlike aggregate structure. This can be taken as further support for the assumption of ascribing τ_c^s to the translational diffusion.

A better description of the relaxation in terms of lateral diffusion from these continuous cubic phases should be given by a random-walk model of the diffusion on a surface equivalent to the proposed model for the aggregate structure. Structural information would thereby be obtained by fitting the dimension of the cubic unit cell to the value of $\tilde{J}_s(0) + \tilde{J}_s(\omega_0) - 2\tilde{J}_s(2\omega_0)$ in eq 5. Computer simulations along these lines are currently being carried out.

Acknowledgment. Thanks are due to Bertil Halle and to Håkan Wennerström for valuable discussions. This work was supported by the Swedish Natural Science Research Council and by the Foundation of "Bengt Lundqvists Minne" (P.O.E.).

Patterns of Three-Liquid-Phase Behavior Illustrated by Alcohol–Hydrocarbon–Water–Salt Mixtures

B. M. Knickerbocker,† C. V. Pesheck,* H. T. Davis, and L. E. Scriven

Department of Chemical Engineering and Materials Science, University of Minnesota, Minneapolis, Minnesota 55455
(Received: June 16, 1981; In Final Form: October 5, 1981)

Ten salts were each dissolved in water and the solutions mixed with equal volumes of one of six hydrocarbons and one of ten monohydric alcohols. The resulting multiphase mixtures were examined for the number of coexisting liquid phases and, in some cases, for the partitioning of alcohol among them. Several unusual patterns of phase behavior have been observed. For example, increasing concentrations of sodium chloride induce the widely observed $\underline{2}3\bar{2}$ pattern of phase behavior in equal-volume mixtures of *n*-propyl alcohol, octane, and brine.[1] However, with lithium chloride, calcium chloride, or magnesium chloride, the induced pattern is $\underline{2}3\bar{3}$. All of the patterns observed in the alcohol–hydrocarbon–brine systems chosen for this study can be summarized by two basic quaternary phase diagrams. It is conjectured that any three- or four-component system exhibiting three liquid phases in equilibrium can be described in terms of these two basic phase diagrams.

Introduction

The phase behavior of alcohol–hydrocarbon–brine mixtures is made rich and varied by hydrogen bonding and other effects of polar intermolecular forces in water and salt solutions, nonpolar forces in hydrocarbons, and both types in alcohols, which are amphiphilic. The dynamic structures caused by hydrogen bonding and other polar interactions make these mixtures difficult to model thermodynamically with empirical equations of solution state, much less in terms of statistics of molecular mechanics. A useful step toward understanding the thermodynamics of such mixtures is to profile their phase behavior experimentally, as we did for certain systems with sodium chloride.[1] In this paper we take up other salts and the basic features of all of the phase diagrams.

As amphiphiles, the lower molecular weight monohydric alcohols employed here can be considered to be protosurfactants even though they form neither micelles nor liquid crystals in aqueous solutions and so display neither property often taken to distinguish surfactants.[2] Previously we reported[1] that numerous alcohol–hydrocarbon–water–sodium chloride mixtures mimic the phase behavior of surfactant–oil–water–salt systems, including those encountered in certain surfactant-based processes for enhancing petroleum recovery. At low salinities, certain mixtures of alcohol, hydrocarbon, and brine split into two phases with most of the alcohol in the lower water-rich phase. At intermediate salinities the split in many instances is into three phases, the alcohol residing chiefly in the middle phase, which also contains substantial fractions of water and hydrocarbon. At higher salinities the split is into two phases with most of the alcohol in the upper, hydrocarbon-rich phase. This so-called $\underline{2}3\bar{2}$ pattern is typical of surfactant–oil–water–salt systems, but our results showed that the pattern is not restricted to amphiphiles which are highly surface active.

In what follows we show that, whereas systems with potassium chloride, sodium sulfate, and sodium bromide also follow the $\underline{2}3\bar{2}$ pattern, those with lithium chloride, magnesium chloride, and calcium chloride behave somewhat differently. Notwithstanding the differences, all

† Mobil Research and Development Corp. Paulsboro, NJ 08066.

(1) B. M. Knickerbocker, C. V. Pesheck, L. E. Scriven, and H. T. Davis, *J. Phys. Chem.*, 83, 1984 (1979).
(2) R. G. Laughlin, *Adv. Liq. Cryst.*, 3, 99 (1978).

0022-3654/82/2086-0393$01.25/0